PHYSICAL REVIEW B **82**, 184115 (2010)

High-pressure phase transformations in carbonates

Sergiu Arapan[1,2,*] and Rajeev Ahuja[1,3]
[1]*Department of Physics and Astronomy, Division of Materials Theory, Uppsala University, P.O. Box 530, S-751 21 Uppsala, Sweden*
[2]*Institute of Electronic Engineering and Industrial Technologies, Academy of Sciences of Moldova,*
Academiei 3/3, MD-2028 Chişinău, Moldova
[3]*Applied Materials Physics, Department of Materials and Engineering,*
Royal Institute of Technology (KTH), S-100 44 Stockholm, Sweden
(Received 4 August 2010; published 22 November 2010)

High-pressure phase transitions sequences in $CaCO_3$, $SrCO_3$, and $BaCO_3$ are studied by first-principle electronic structure calculations. Each of the carbonates undergoes the *aragonite* to *postaragonite* phase transition with pressure in agreement with the experimental observation of Ono *et al.* However, the *postaragonite* to *post-postaragonite* phase transition, predicted by Oganov *et al.* and later observed in $CaCO_3$, is unlikely to occur in $SrCO_3$ and $BaCO_3$. Hence, the concept that isostructural compounds will exhibit the same type of pressure-induced phase transitions has limitations. A change of the hybridization of the carbon atom from sp^2 to sp^3 within the *Pmcn* phase occurs in each of compounds, thus the carbonates are likely to transform at very high pressure to structures with tetrahedral CO_4^{-4} carbonate group.

DOI: 10.1103/PhysRevB.82.184115 PACS number(s): 91.60.Hg, 91.60.Gf, 91.60.Ed

I. INTRODUCTION

The question of stability of the subducted carbonates has received a considerable attention during the last decade. Such an interest is motivated by the understanding of the processes of carbon recycling at the boundary between lithosphere and asthenosphere of the Earth's mantle and the possibility to store carbon in the form of a compound stable at pressure and temperature corresponding to the Earth's mantle conditions. The content of carbon in the exosphere is small compared to the total amount of carbon our planet might contain and this imply that most of carbon might be present in the Earth' mantle.[1–4] A possible mechanism of removing carbon from the exosphere and delivering it deep into the mantle of the Earth is the subduction of carbonates.[5] Although carbonates minerals are minor components in the Earth's mantle, $MgCO_3$ and $CaCO_3$ are the most abundant carbon bearing phases within the interior of the Earth. Despite the fact that recent experiments impose some constraints on the subduction of carbonates into the lower mantle,[6] there are experimental evidences that $MgCO_3$ is stable at the Earth's lower mantle conditions,[7] and that carbonates could be recycled into the lower mantle by subducted oceanic crust.[8]

At ambient conditions magnesite $MgCO_3$, calcite $CaCO_3$ and dolomite $CaMg(CO_3)_2$ are the stable phases of Mg-and Ca-bearing carbonates. At pressures corresponding to the Earth's upper mantle conditions calcite transforms to aragonite,[9] and dolomite breaks down into magnesite and aragonite at pressures corresponding to the boundary between the Earth's crust and upper mantle.[10,11] At higher pressures both magnesite and aragonite are likely to transform to other phases and the determination of possible high-pressure phases of carbonates has stimulated a series of both experimental and theoretical investigations. Originally Lin and Liu[12,13] have reported identical phase transitions in aragonite-type carbonates $BaCO_3$ (witherite) and $SrCO_3$ (strontianite) to occur at 8 and 35 GPa, respectively. Quenched at ambient pressure conditions, these compounds exhibited an orthorhombic phase with space group $P2_122$, and a unit cell dimensionally similar to the aragonite structure of these minerals, but with doubled *a* and *b* axes. Holl *et al.*[14] have also reported a phase transformation in $BaCO_3$ at 7.3 GPa and by *in situ* single-crystal x-ray diffraction have refined the new structure in space group $P\bar{3}1c$. Although $BaCO_3$ and $SrCO_3$ are not the compounds of geophysical interest, high-pressure study of these minerals was motivated by the idea that isostructural compounds should exhibit similar phase transformations. Since the cation radius of Ba is larger than that of Sr and Ca, then any pressure induced transformation that occurs in aragonite should also occur in witherite, but at lower pressure. And, indeed, Santillan and Williams[15] reported phase transformations similar to that observed in $BaCO_3$ by Holl *et al.* to occur in $CaCO_3$ at pressure of 50 GPa. At the same time, Ono *et al.*[16–18] have reported distinctly different results. They also observed structural phase transition to occur in $CaCO_3$ at 40 GPa, and in $SrCO_3$ and $BaCO_3$ at 10 GPa, but the postaragonite structure was determined as an orthorhombic phase. As for $MgCO_3$, Isshiki *et al.*[19] have found the magnesite phase to be stable up to 115 GPa. Above 115 GPa $MgCO_3$ undergoes a transition to a new structure, which, surprisingly, seems to be different than that of aragonite.

In a recent theoretical study by Skorodumova *et al.*,[20] based on first-principle calculations, magnesite has been found to transform into a pyroxene structure (space group $C2/c$) at 113 GPa, which subsequently transforms into the $CaTiO_3$-type structure (space group *Pmcn*) at 200 GPa. The postaragonite structure observed by Ono *et al.*,[16] was predicted in $CaCO_3$ by Oganov *et al.*[21] by using first principle calculations in combination with evolutionary structure predicting algorithms.[22] By means of electronic structure calculations the correct postaragonite phase has been refined in space group *Pmmn*. Moreover, with the help of newly designed universal structure predicting method USPEX, Oganov *et al.*[21] have predicted a postaragonite to post-postaragonite phase transition at 137 GPa, experimentally confirmed later.[24] The high-pressure polymorph of $CaCO_3$ above 137 GPa is a pyroxene-type structure in space group $C222_1$ and Oganov *et al.*[21] have found this structure to be the stable structure of $MgCO_3$ at high pressure. Shortly after, a more rigorous search of low-enthalpy structures by using USPEX has revealed the existence of two new thermodynamically stable phases of $MgCO_3$ at pressures above 82 GPa.[23] It has been found that between 82.4 and 138.1 GPa the most stable structure of $MgCO_3$, called phase II, has space group $C2/m$ with 30 atoms in the primitive cell. Above 138.1 GPa another structure, denoted phase III, with space group $P2_1$ and 30 atoms in the unit cell becomes more stable. Although high-pressure experiments could not identify these phases, the x-ray diffraction patterns can be explained by a mixture of magnesite and these new phases.

These new predicted structures are formidable in the sense that they contain chains ($C222_1$) or rings ($C2/m,P2_1$) of tetrahedral carbonate groups CO_4^{4-} in sharp contrast to the parallel arrangement of triangular CO_3^{2-} carbonate groups of the aragonite and postaragonite phases. High-pressure phases are, thus, qualitatively different and correspond to a different chemical regime. Arapan *et al.* have shown[25] that this transition is due to the change of carbon's hybridization state. In their numerical simulations they observed a transition from sp^2 to sp^3 hybridized carbon state within the *Pmcn* crystal structure. Moreover, this new high-pressure modified or overcompressed aragonite structure becomes even more stable than the pyroxene structure $C222_1$ above 240 GPa. We show in Fig. 1 the high-pressure phase sequence of $CaCO_3$.

We have also investigated whether similar phase transitions sequences occur in $SrCO_3$ and $BaCO_3$ carbonates, and in this paper we give the results of this study. First, our results show that each of the carbonates undergoes the phase transition from the aragonite to the postaragonite structure reported by Ono *et al.* However, $SrCO_3$ and $BaCO_3$ do not follow the same structural changes as $CaCO_3$ at higher pressures, and the pyroxene structure $C222_1$ do not appear in these two compounds. A similar result has been shown recently for $BaCO_3$.[26] Second, we have obtained the sp^2 to sp^3 transition of the carbon hybridization state in both $SrCO_3$ and $BaCO_3$, but at larger pressures than in $CaCO_3$. Subsequently, the overcompressed aragonite structure becomes more stable than postaragonite one at very high pressures: above 265 GPa in $SrCO_3$, and above 296 GPa in $BaCO_3$. Thus, the concept that isostructural compounds will exhibit the same type of pressure-induced phase transitions is valid only for the aragonite to postaragonite phase transition, and can be applied for a certain pressure range only. In the fol-

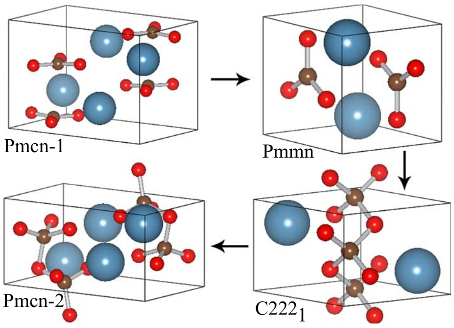

FIG. 1. (Color online) Phase transformations sequence of $CaCO_3$ at high pressure: aragonite (*Pmcn*-1)→postaragonite (*Pmmn*)→post-post-aragonite ($C222_1$)→overcompressed aragonite (*Pmcn*-2).

TABLE I. Structure parameters (lattice constants and Wyckoff positions $4c(1/4,y,z)$ and $8d(x,y,z)$ of nonequivalent atoms) of the *aragonitePmcn*-1 phase. $M=(\mathrm{Ca},\mathrm{Sr},\mathrm{Ba})$.

		$CaCO_3$	$SrCO_3$	$BaCO_3$
a b c		4.9598 7.9641 5.7379[a]	5.1059 8.4207 6.0319[b]	5.3103 8.9122 6.4365[c]
	PBE	5.0122 8.0268 5.8083	5.1625 8.4934 6.1352	5.3729 8.9973 6.5928
	PW91	4.9970 8.0110 5.7841	5.1493 8.4782 6.1060	5.3620 8.9842 6.5596
M (4*c*)		0.5851 0.2597[a]	0.5840 0.2569[d]	0.5838 0.2556[c]
	PBE	0.5851 0.2593	0.5838 0.2564	0.5836 0.2543
	PW91	0.5850 0.2591	0.5838 0.2563	0.5835 0.2544
C (4*c*)		0.2386 0.4148[a]	0.2399 0.4136[d]	0.2566 0.4289[c]
	PBE	0.2378 0.4166	0.2413 0.4171	0.2434 0.4220
	PW91	0.2380 0.4160	0.2414 0.4165	0.2434 0.4213
O1 (4*c*)		0.0770 0.4043[a]	0.0881 0.4054[d]	0.0989 0.4225[c]
	PBE	0.0771 0.4072	0.0886 0.4081	0.0988 0.4145
	PW91	0.0775 0.4066	0.0889 0.4075	0.0991 0.4139
O2 (8*d*)		0.4737 0.3196 0.4131[a]	0.4694 0.3179 0.4161[d]	0.4654 0.3195 0.4212[c]
	PBE	0.4740 0.3197 0.4140	0.4680 0.3183 0.4160	0.4600 0.3159 0.4217
	PW91	0.4740 0.3197 0.4135	0.4679 0.3182 0.4155	0.4597 0.3158 0.4210

[a] Reference 33 (experiment).
[b] Reference 34 (experiment).
[c] Reference 35 (experiment).
[d] Reference 36 (experiment).

TABLE II. Structure parameters (lattice constants and Wyckoff position $6h(x,y,1/4)$ of the O atom) of the $P\bar{3}c1$ phase.

		$CaCO_3$(50 GPa)	$SrCO_3$(10 GPa)	$BaCO_3$(8.2 GPa)
a c		4.58 4.55^{a}		5.30 5.19^{b}
	PBE	4.5994 4.3547	5.0591 5.0073	5.3560 5.1540
	PW91	4.5951 4.3540	5.0520 4.9930	5.3493 5.1405
O (6*h*)				0.140 0.860^{b}
	PBE	0.1603 0.8499	0.1482 0.8557	0.1409 0.8630
	PW91	0.1601 0.8501	0.1480 0.8559	0.1407 0.8632

[a] Reference 15 (experiment).
[b] Reference 14 (experiment).

lowing sections we will describe the details of our calculations and discuss our results.

II. DETAILS OF CALCULATIONS

These calculations were done by using VASP,[27] which is an implementation of the projector augmented-wave method (PAW) within the density functional theory (DFT). We used the PAW potentials[28,29] derived within the generalized gradient approximation (GGA) description of the electronic exchange-correlation effects. We performed calculations by using two types of GGA PAW potentials: potentials with the Perdew-Wang parametrization of the exchange-correlation functional (PW91)[30] and the Perdew-Burke-Ernzerhofe approximation (PBE).[31] For both types of potentials we considered $3s^2 3p^6 4s^2$, $4s^2 4p^6 5s^2$, and $5s^2 5p^6 6s^2$ orbitals as valence states for Ca, Sr, and Ba, respectively. For carbon $2s^2 2p^2$ orbitals and for oxygen $2s^2 2p^4$ orbitals where treated as valence states. In the case of the PW91 potentials we used the so called "hard" potentials with $r_{core}=1.10$ a.u. for C and O, and for the PBE potentials we used potentials with $r_{core}=1.50$ a.u. for C and with $r_{core}=1.52$ a.u. for O. Initially, the use of "hard" potentials was motivated by performing calculations at pressures higher than 300 GPa. However, in our paper[25] we obtained a transition pressure different from that predicted by Oganov *et al.*[21] for the postaragonite *Pmmn* phase to the pyroxene-type phase $C222_1$ transformation. Since the transition from postaragonite to $C222_1$ structure has been observed at the predicted pressure, we performed additional calculations using the same PBE potentials as in Ref. 21. All considered structure were optimized at each volume until the Hellmann-Feynman forces became less than 1 meV/Å and a cutoff energy larger by a factor of 1.5 than the default cutoff energy where used to ensure a convergence within 1 meV/atom of the total energy with respect to the number of plane waves in the basis set. We used a fully automatic scheme, which generates Γ centered Monkhorst-Pack grid with equally spaced *k*-points, to sample the Brillouin zone and we used the same density of *k*-points at different volumes. In such a way we ensured the same degree of convergence with respect to reciprocal space vectors at different pressures.

III. RESULTS AND DISCUSSION

In our investigation of the high-pressure phase transformations sequence in $CaCO_3$, $SrCO_3$, and $BaCO_3$ carbonates we considered structures observed in experiment[14–18] and predicted in previous numerical simulations.[21,25] At low pressures all three compounds are stable in the structure of aragonite (*Pmcn*-1), which has an orthorhombic symmetry and

TABLE III. Structure parameters (lattice constants and Wyckoff positions $2a(0,0,z)$, $2b(0,1/2,z)$, and $4e(0,y,z)$ of nonequivalent atoms) of the *postaragonite Pmmn* phase. $M=(\mathrm{Ca},\mathrm{Sr},\mathrm{Ba})$.

		$CaCO_3$(66.4 GPa)	$SrCO_3$(14.5 GPa)	$BaCO_3$(70 GPa)
a b c		4.101 4.561 3.964^{a}	4.652 5.043 4.309^{b}	4.255 4.895 4.255^{c}
	PBE	4.0664 4.5956 3.9914	4.6625 5.1014 4.3476	4.2758 4.9489 4.2876
	PW91	4.0633 4.5886 3.9860	4.6499 5.0926 4.3398	4.2740 4.9460 4.2837
M (2*b*)		0.6230^{a}		0.6176^{c}
	PBE	0.6218	0.6167	0.6176
	PW91	0.6217	0.6167	0.6173
C (2*a*)		0.9904^{a}		0.9865^{c}
	PBE	0.9910	0.9915	0.9865
	PW91	0.9910	0.9914	0.9866
O1 (2*a*)		0.6700^{a}		0.6921^{c}
	PBE	0.6725	0.6934	0.6921
	PW91	0.6730	0.6937	0.6928
O2 (4*e*)		0.2398 0.1473^{a}		0.2209 0.1357^{c}
	PBE	0.2378 0.1482	0.2191 0.1383	0.2209 0.1358
	PW91	0.2373 0.1479	0.2187 0.1381	0.2203 0.1354

[a] Reference 21 (experiment and calculations).
[b] Reference 17 (experiment).
[c] Reference 26 (calculations).

TABLE IV. Structure parameters (lattice constants and Wyckoff positions $4a(x,0,0)$, $4b(0,y,\frac{1}{4})$, and $8c(x,y,z)$ of nonequivalent atoms) of the *post-post-aragonite* $C222_1$ phase. $M=(\mathrm{Ca},\mathrm{Sr},\mathrm{Ba})$.

		$CaCO_3$(152.2 GPa)	$SrCO_3$(180 GPa)	$BaCO_3$(70 GPa)
a b c		5.544 6.926 3.213[a]		
	PBE	5.5491 6.9082 3.2072	5.8000 6.9040 3.2346	6.3369 8.0916 3.5109
	PW91	5.5453 6.9036 3.2053	5.7981 6.9021 3.2321	6.3371 8.0876 3.5054
M (4*b*)		0.8287[b]		
	PBE	0.8292	0.8404	0.8339
	PW91	0.8292	0.8404	0.8339
C (4*a*)		0.3538[b]		
	PBE	0.3541	0.3627	0.3706
	PW91	0.3541	0.3627	0.3705
O1 (4*b*)		0.3881[b]		
	PBE	0.3879	0.3872	0.4011
	PW91	0.3880	0.3874	0.4013
O2 (8*c*)		0.2736 0.3875 0.7324[b]		
	PBE	0.2733 0.3872 0.7323	0.2567 0.3877 0.7342	0.2405 0.3995 0.7165
	PW91	0.2730 0.3874 0.7318	0.2564 0.3879 0.7337	0.2403 0.3997 0.7161

[a] Reference 24 (experiment).

[b] Reference 21 (calculations).

four formula units.[32] The symmetry of the aragonite structure is described by space group *Pmcn* with cation and carbon atoms at 4*c* Wyckoff site, and oxygen atoms at 4*c* and 8*d* Wyckoff positions. Lattice parameters and Wyckoff positions for different atomic species in the *Pmcn*-1 structure at ambient pressure are shown in Table I. Calculated atomic positions are in excellent agreement with the experimental observation and are almost the same for two different type of potentials. Data for lattice parameters are in good agreement with the experimental one, being slightly larger since the GGA exchange-correlation functional overestimates the equilibrium volume. One may also notice that different potentials give slightly different results for lattice parameters.

The aragonite-type carbonates undergo a phase transition to a postaragonite phase. In our calculations we have considered both postaragonite structures observed in experiment. The postaragonite structure observed by Holl *et al.*[14] has a trigonal symmetry and two formula units, with cation atoms at $2d(2/3,1/3,1/4)$ site, carbon atoms at $2a(0,0,1/4)$ site and oxygen atoms at 6*h* Wyckoff site in space group $P\bar{3}1c$. The postaragonite structure observed by Ono *et al.*[16] and predicted by Oganov *et al.*[21] has an orthorhombic symmetry and two formula units, with cation atom at 2*b* position, carbon atoms at 2*a* Wyckoff site, and oxygen atoms at 2*a* and 4*e* Wyckoff sites in space group *Pmmn*. Lattice parameters and Wyckoff positions in the $P\bar{3}1c$ and *Pmmn* structures are shown in Tables II and III, respectively.

The next phase considered in the phase transition sequence is the post-post-aragonite phase predicted in $CaCO_3$ by Oganov *et al.*[21] and experimentally confirmed by Ono *et al.*[24] This phase has an orthorhombic symmetry with a *C*-face centered Bravais lattice and cation atoms at 4*b* site, carbon atoms at 4*a* site, and oxygen atoms at 4*b* and 8*c* Wyckoff sites in space group $C222_1$. And, finally we consid-

TABLE V. Structure parameters (lattice constants and Wyckoff positions $4c(1/4,y,z)$ and $8d(x,y,z)$ of nonequivalent atoms) of the *overcompressed-aragonite* *Pmcn*-2 phase. $M=(\mathrm{Ca},\mathrm{Sr},\mathrm{Ba})$.

		$CaCO_3$(250 GPa)	$SrCO_3$(280 GPa)	$BaCO_3$(280 GPa)
a b c	PBE	4.2544 7.0861 3.5761	4.3568 7.2189 3.6525	4.5590 7.5474 3.7674
	PW91	4.2500 7.0875 3.5752	4.3537 7.2206 3.6513	4.5571 7.5518 3.7661
M (4*c*)	PBE	0.6134 0.1621	0.6171 0.1527	0.6152 0.1312
	PW91	0.6135 0.1622	0.6171 0.1524	0.6151 0.1307
C (4*c*)	PBE	0.3230 0.4524	0.3230 0.4591	0.3222 0.4757
	PW91	0.3230 0.4515	0.3231 0.4585	0.3222 0.4753
O1 (4*c*)	PBE	0.1398 0.3281	0.1433 0.3299	0.1517 0.3382
	PW91	0.1402 0.3272	0.1437 0.3293	0.1521 0.3381
O2 (8*d*)	PBE	0.5121 0.3789 0.3291	0.5017 0.3811 0.3371	0.4878 0.3806 0.3590
	PW91	0.5115 0.3790 0.3288	0.5012 0.3811 0.3373	0.4873 0.3805 0.3597

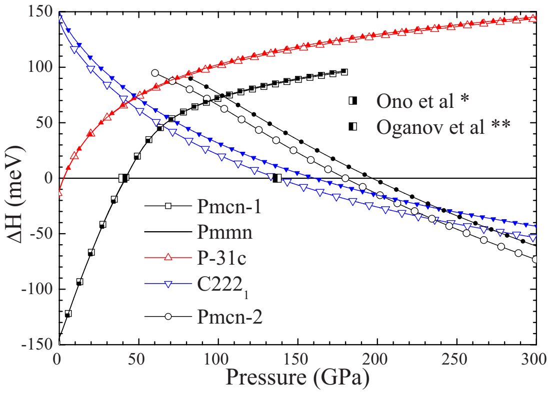

FIG. 2. (Color online) Enthalpy of different $CaCO_3$ phases with respect to the postaragonite *Pmmn* phase versus pressure. The results of calculations performed with the PBE potentials are shown by large open symbols and the results obtained with the PW91 "hard" potentials are shown by filled small symbols. Half-open symbols show the experimentally observed transition pressures: * = [16], ** = [21].

ered the overcompressed aragonite structure (*Pmcn*-2),[25] which has the same symmetry as the aragonite structure. Calculated and experimentally observed lattice parameters and Wyckoff positions in the $C222_1$ and *Pmcn*-2 structures are shown in Tables IV and V, respectively.

A. Phase diagram of $CaCO_3$

In Fig. 2 the phase diagram of $CaCO_3$ at $T=0$ K is shown. Enthalpies of different phases are shown with respect to the enthalpy of the postaragonite structure *Pmmn*. First, we observe that the transition pressures of the aragonite to postaragonite *Pmmn* phase and of the *Pmmn* to pyroxene-type structure $C222_1$ are in excellent agreement with the experimentally observed values and those predicted by previous calculations. Second, we see that the results of the calculations performed with the PW91 "hard" potentials differ from those done with the PBE potentials for structures with CO_4^{4-} tetrahedral carbonate group only. Since the main difference is the use of "hard" potentials for C and O atoms, we have an implicit proof of the fact that at high pressures the structural changes are mainly determined by the change in the chemistry of the carbonate group. For numerical simulations performed with the PBE potentials the transition from pyroxene-type phase $C222_1$ to the overcompressed aragonite structure *Pmcn*-2 occurs at 235 GPa (240 GPa with "hard" potentials). The change of the hybridization state of carbon from sp^2 to sp^3 within the *Pmcn* structure occurs at 95 GPa (103 GPa with "hard" potentials). Thus, for $CaCO_3$ the aragonite structure *Pmcn*-1 is stable up to 41.5 GPa, postaragonite structure *Pmmn* is stable from 41.5 to 137 GPa, the post-post-aragonite structure $C222_1$ is stable form 137 GPa to 235 GPa, and the overcompressed aragonite structure *Pmcn*-2 becomes stable above 235 GPa.

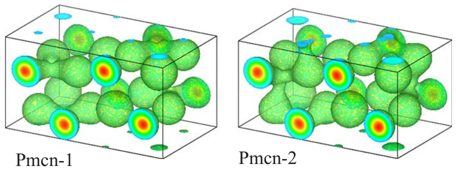

FIG. 4. (Color online) Isosurfaces of the electronic charge density distribution for the aragonite (*Pmcn*-1) and overcompressed aragonite (*Pmcn*-2) at about 200 GPa

Despite the striking structural similarities between the aragonite and overcompressed aragonite (both structures are characterized by the same space group *Pmcn*, with atoms in the same Wyckoff positions, and similar lattice parameters), these two phases are different with quite distinct electronic structure (Fig. 3). Different electronic structures for almost similar atom arrangements and lattice parameters are due to change in the distribution of the charge density that accompanies the change of the hybridization state of C (Fig. 4).

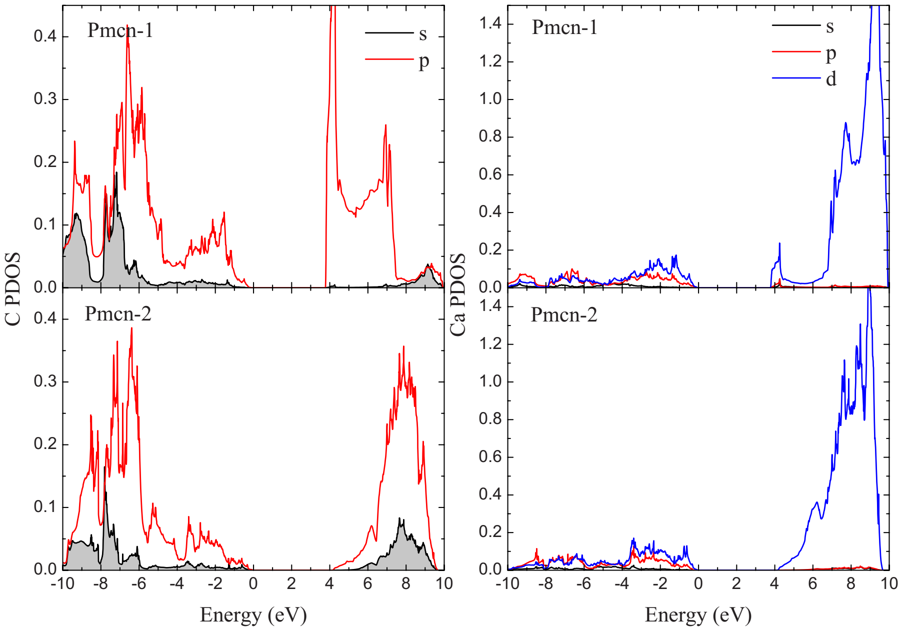

FIG. 3. (Color online) Partial density of states PDOS of C and Ca atoms for the aragonite (*Pmcn*-1) and overcompressed aragonite (*Pmcn*-2) phases at pressure close to 200 GPa.

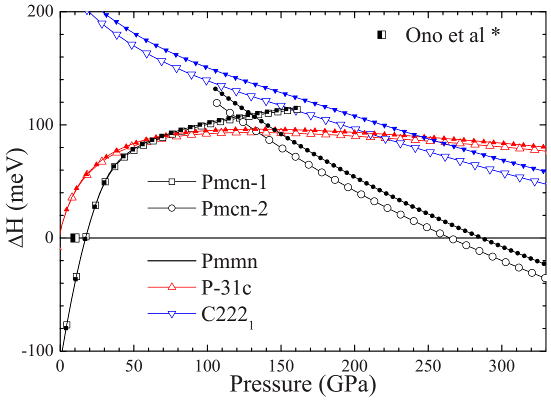

FIG. 5. (Color online) Enthalpy of different $SrCO_3$ phases with respect to postaragonite *Pmmn* phase as a function of pressure. Notations are the same as in Fig. 2. *= **17**.

B. Phase diagrams of $SrCO_3$ and $BaCO_3$

In Fig. 5 we show the phase diagram of $SrCO_3$ calculated at $T=0$ K for two sets of the PAW potentials. We confirm for the postaragonite phase the *Pmmn* structure determined by Ono *et al.*[17] The transition from the aragonite to postaragonite structure occurs at a pressure of 17 GPa, higher than the transition pressure of 10 GPa observed in the experiment. We also see that two sets of the PAW potentials give different results for the high-pressure phases with tetrahedral carbonate group. However, the most unexpected result is that the transition from the *Pmmn* to $C222_1$ structure does not occur in $SrCO_3$. In contrast to the pyroxene-type structure, the overcompressed aragonite phase becomes more stable than the postaragonite *Pmmn* structure at pressures above 265 GPa. We also observe the change of the hybridization state of carbon in the *Pmcn* structure at 120 GPa.

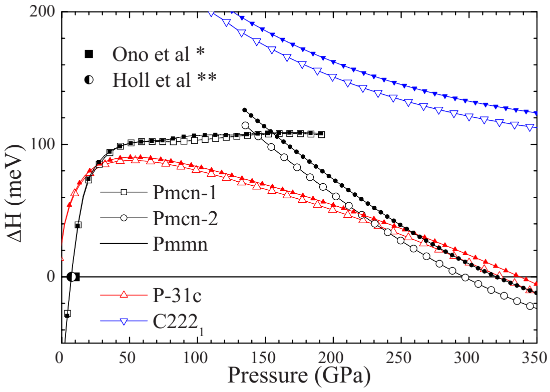

FIG. 6. (Color online) Enthalpy of different $BaCO_3$ phases with respect to the postaragonite *Pmmn* phase as a function of pressure. Notations are the same as in Fig. 2. *= [18], **= [14].

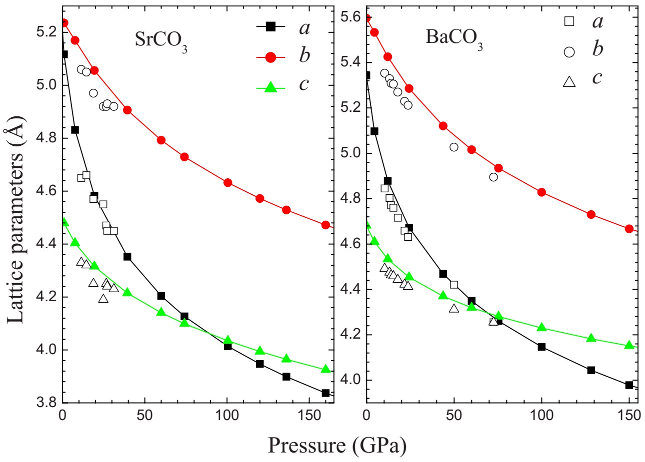

FIG. 7. (Color online) Lattice parameters of the postaragonite phase of $SrCO_3$ and $BaCO_3$ as a function of pressure. Filled symbols correspond to *ab initio* calculations, while open symbols are experimental results of Ono *et al.*:[17] for $SrCO_3$ and Ono[18] for $BaCO_3$.

The phase diagram of $BaCO_3$ obtained at $T=0$ K is shown in Fig. 6. The calculations done for two different sets of PAW potentials give similar results for structures with CO_3^{2-} carbonate groups, however there is a small difference at high pressure for the trigonal phase $P\bar{3}1c$. The results differ considerably for structures containing CO_4^{4-} carbonate groups. In the case of $BaCO_3$, the transition from aragonite to postaragonite occurs at 7 GPa in excellent agreement with the experimental finding of Holl *et al.*[14] and in good agreement with experimental transition pressure of 10 GPa reported by Ono *et al.*[18] The postaragonite phase is the *Pmmn* structure and, as in the $SrCO_3$, this phase has a very large stability field. The pyroxene-type structure $C222_1$ appears to be energetically unfavorable within the whole interval of pressures, while the overcompressed aragonite structure becomes stable above 296 GPa. The transition from sp^2 to sp^3 carbon hybridized state in the carbonate groups of the *Pmcn* structure occurs at 144 GPa.

At this point we can draw three conclusions from our results. First, the postaragonite structure in these carbonates is the structure observed by Ono *et al.*[16–18] and predicted by Oganov *et al.*[21] Second, the phase transitions sequence in $SrCO_3$ and $BaCO_3$ is different than the phase transformations sequence in $CaCO_3$ at pressures higher than the transition pressure to postaragonite phase. The pyroxene-type structure $C222_1$, that exists at high-pressure in $CaCO_3$,[21,24] does not exists in $SrCO_3$ and $BaCO_3$. Finally, the change of the carbon hybridization within the *Pmcn* structures occurs in each of the compounds and the overcompressed aragonite structure with CO_4^{4-} carbonate groups is the stable structure at very high pressure.

It is remarkable the fact that the postaragonite phase *Pmmn* is thermodynamically stable within a large interval of pressures in both $SrCO_3$ and $BaCO_3$. One can also notice, that the compressibility of the postaragonite structure shows a significant anisotropy under applied hydrostatic pressure (Fig. 7). Thus, the *Pmmn* phase is more compressible along the direction normal to cation and CO_3 group planes, which corresponds to the *a* axis. Due to this anisotropy, the *a* axis becomes shorter than the *c* one with pressure,[26] and at some given pressures, about 90 and 70 GPa for $SrCO_3$ and $BaCO_3$, respectively, their lengths should become equal.

The results of our investigation show that the concept that isostructural compounds will exhibit the same type of pressure-induced phase transitions is valid only within a cer-

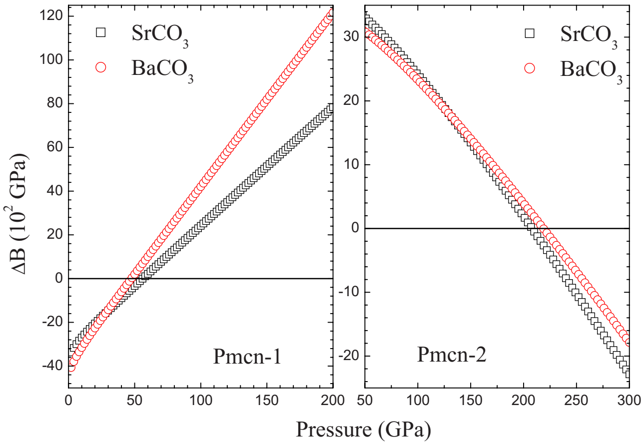

FIG. 8. (Color online) Bulk modulus of $SrCO_3$ and $BaCO_3$ as a function of applied pressure with respect to the bulk modulus of $CaCO_3$ for the aragonite and overcompressed aragonite phases.

tain range of pressures. In the case of $CaCO_3$, $SrCO_3$, and $BaCO_3$ carbonates it works only for pressures at which the aragonite to postaragonite transformation occurs. In both Sr and Ba atoms the valence electrons are spread at large distance around the core ionic shell and, in compounds, Sr and Ba atoms are characterized by an increased cation polarizability.[37] Therefore, at moderate pressures $SrCO_3$ and $BaCO_3$ are easy to compress. In Fig. 8 the bulk modulus $B = B(P)$ for the aragonite and overcompressed aragonite phases of $SrCO_3$ and $BaCO_3$ with respect to the bulk modulus of the same phases of $CaCO_3$ is shown as a function of pressure. For the aragonite structure *Pmcn*-1 we clearly see the change in the compressibility for each of the carbonates and the reverse of the order of compounds with respect to the degree of compressibility at high pressures. Hence, one might expect a phase transformation to occur in carbonates, with respect to the transition pressure, in the following order: $BaCO_3$, $SrCO_3$, and $CaCO_3$. However, as the pressure increases and the density of valence electrons within the semicore region increases, Sr and Ba become less compressible. For the overcompressed aragonite structure *Pmcn*-2, in contrast to aragonite structure, $BaCO_3$ and $SrCO_3$ are less compressible than $CaCO_3$ and the order of compounds according to the degree of compressibility reverses at very high pressure when this structure becomes stable. Thus, the transition to overcompressed aragonite in carbonates should occur, with respect to the transition pressure, in the following order: $CaCO_3$, $SrCO_3$, and $BaCO_3$. Both these conclusions are supported by our calculations as well as experimental data.

IV. SUMMARY

By performing first-principle electronic structure calculations we show that $CaCO_3$, $SrCO_3$, and $BaCO_3$ carbonates undergo the same kind of aragonite to post aragonite transformation and confirm the experimental results of Ono *et al.*[16–18] We also show that the concept that isostructural compounds with different cations undergo the same phase transitions sequence can be applied only within a certain range of pressures. We cannot predict the phase transformations sequence in all compounds by generalizing the results obtained for the compound with the largest cation radius at all pressures. Thus, the pyroxene-type structure $C222_1$ predicted and experimentally confirmed in $CaCO_3$ (Refs. 21 and 24) do not exist in $SrCO_3$ and $BaCO_3$. However, we show that the change of carbon hybridization state from sp^2 to sp^3 does occur in each of these compounds and the overcompressed aragonite structure predicted in $CaCO_3$ (Ref. 25) becomes stable in $SrCO_3$ and $BaCO_3$ at very high pressures.

ACKNOWLEDGMENTS

Calculations were performed using the UPPMAX and NSC computer facilities. We acknowledge the financial support from the Swedish Research Council (VR). We would like to thank Natalia V. Skorodumova for valuable discussions regarding the compressibility of the earth-alkaline element in various compounds and Artem R. Oganov for a very important discussion about the use of different PAW potentials.

---

*sergiu.arapan@fysik.uu.se

[1] B. Marty and A. Jambon, Earth Planet. Sci. Lett. **83**, 16 (1987).

[2] G. W. Berg, Nature (London) **324**, 50 (1986).

[3] B. J. Wood, A. Pawley, and D. R. Frost, Philos. Trans. R. Soc. London, Ser. A **354**, 1495 (1996).

[4] E. J. Garnero, Science **304**, 834 (2004).

[5] H. Becker and R. Altherr, Nature (London) **358**, 745 (1992).

[6] T. Hammouda, Earth Planet. Sci. Lett. **214**, 357 (2003).

[7] C. Biellman, Ph. Gillet, F. Guyot, J. Peyronneau, and B. Reynard, Earth Planet. Sci. Lett. **118**, 31 (1993).

[8] K. Hoernle, G. Tilton, M. J. Le Bas, S. Duggen, and D. Garbe-Schönberg, Contrib. Mineral. Petrol. **142**, 520 (2002).

[9] K. Suito, J. Namba, T. Horikawa, Y. Taniguchi, N. Sakurai, M. Kobayashi, A. Onodera, O. Shimomura, and T. Kikegawa, Am. Mineral. **86**, 997 (2001).

[10] K. Sato and T. Katsura, Earth Planet. Sci. Lett. **184**, 529 (2001).

[11] M. Shirasaka, E. Takahashi, Y. Nishihara, K. Matsukage, and T. Kikegawa, Am. Mineral. **87**, 922 (2002).

[12] C. C. Lin and L. G. Liu, J. Phys. Chem. Solids **58**, 977 (1997).

[13] C. C. Lin and L. G. Liu, Phys. Chem. Miner. **24**, 149 (1997).

[14] C. M. Holl, J. R. Smyth, H. M. S. Lautsen, S. D. Jacobsen, and R. T. Downs, Phys. Chem. Miner. **27**, 467 (2000).

[15] J. Santillán and Q. Williams, Am. Mineral. **89**, 1348 (2004).

[16] S. Ono, T. Kikegawa, Y. Ohishi, and J. Tsuchiya, Am. Mineral. **90**, 667 (2005).

[17] S. Ono, M. Shirasaka, T. Kikegawa, and Y. Ohishi, Phys. Chem. Miner. **32**, 8 (2005).

[18] S. Ono, Phys. Chem. Miner. **34**, 215 (2007).

[19] M. Isshiki, T. Irifune, K. Hirose, S. Ono, Y. Ohishi, T. Watanuki, E. Nishibori, M. Takata, and M. Sakata, Nature (London) **427**,

60 (2004).

[20] N. V. Skorodumova, A. B. Belonoshko, L. Huang, R. Ahuja, and B. Johansson, Am. Mineral. **90**, 1008 (2005).

[21] A. R. Oganov, C. W. Glass, and S. Ono, Earth Planet. Sci. Lett. **241**, 95 (2006).

[22] A. R. Oganov and C. W. Glass, J. Chem. Phys. **124**, 244704 (2006).

[23] A. R. Oganov, S. Ono, Y. Ma, C. W. Glass, and A. Garcia, Earth Planet. Sci. Lett. **273**, 38 (2008).

[24] S. Ono, T. Kikegawa, and Y. Ohishi, Am. Mineral. **92**, 1246 (2007).

[25] S. Arapan, J. Souza de Almeida, and R. Ahuja, Phys. Rev. Lett. **98**, 268501 (2007).

[26] S. Ono, J. P. Brodholt, and G. D. Price, Mineral. Mag. **72**, 659 (2008).

[27] G. Kresse and J. Furthmüller, Phys. Rev. B **54**, 11169 (1996).

[28] P. E. Blöchl, Phys. Rev. B **50**, 17953 (1994).

[29] G. Kresse and D. Joubert, Phys. Rev. B **59**, 1758 (1999).

[30] J. P. Perdew, J. A. Chevary, S. H. Vosko, K. A. Jackson, M. R. Pederson, D. J. Singh, and C. Fiolhais, Phys. Rev. B **46**, 6671 (1992).

[31] J. P. Perdew, K. Burke, and M. Ernzerhof, Phys. Rev. Lett. **77**, 3865 (1996).

[32] A. Dal Negro and L. Ungaretti, Am. Mineral. **56**, 768 (1971).

[33] B. Dickens and J. S. Bowen, J. Res. Natl. Bur. Stand., Sect. A **75**, 27 (1971).

[34] J. A. Speer and M. L. Hensley-Dunn, Am. Mineral. **61**, 1001 (1976).

[35] S. M. Antao and I. Hassan, Phys. Chem. Miner. **34**, 573 (2007).

[36] J. P. R. De Villiers, Am. Mineral. **56**, 758 (1971).

[37] N. V. Skorodumova, K. Hermansson, and B. Johansson, Phys. Rev. B **72**, 125414 (2005).